

Cosmic Ray Proton Background Could Explain ATIC Electron Excess

A.R. Fazely,^{*} R.M. Gunasingha,[†] and S.V. Ter-Antonyan
Southern University, Baton Rouge, LA 70813

We show that the excess in the Galactic electron flux recently published by Chang, et al. (Nature, 20 Nov. 2008) can have a simple methodical origin due to a contribution from misidentified proton induced electron-like events in the ATIC detector. A subtraction of the cosmic ray proton component from the published ATIC electron flux eliminates this excess in the range of 300 to 800 GeV.

PACS numbers: 95.30.Cq, 14.80.Ly

An excess in the Galactic electron flux in the range of 300 – 800 GeV recently published by J. Chang, et al, [1] has led to numerous speculations [1, 2, 3, 4, 5, 6, 7] about the origin of the purported excess such as annihilation of dark matter (DM) [1, 2], decaying DM [2, 3], decay of lightest superparticle DM [4], interaction of high energy cosmic rays with photon background near accelerating sites [5], a few nearby SNR [6], and distant young pulsars [7]. All theoretical predictions [1, 2, 3, 4, 5, 6, 7] describe with more or less efficiency the published energy spectrum reported by Chang et al.,[1] in the energy region of 300 – 800 GeV depending on a number of applied free model parameters.

Chang, et al.,[1] use an excess of 70 events, spread over an energy range of 500 GeV, to report a $\sim 6\sigma$ signal based on a 210-event sample, where a background of 140 events was estimated with a GALPROP [8] calculation, neglecting both systematic uncertainties associated with the GALPROP prediction [8] as well as those of the ATIC instrument. Not noted in reference [1], the expected fluctuation of the Galactic electron flux due to the stochastic nature of sources [9, 10] alone could introduce more than a 20% uncertainty for energies above 300 GeV. A major source of background of the ATIC electron experimental data is due to the primary cosmic ray proton component where the bulk of the proton energy is transferred to a single particle, for example, a π^0 in the carbon-scintillator target of the ATIC detector.

In this letter, following the principle of Occam's Razor mentioned in the title of a recent paper by Stefano Profumo [7], we investigated the methodical origin of the reported excess. We studied the contributions due to high energy primary protons and atmospheric e^\pm and γ to the reported Galactic electron flux in the ATIC data. The primary proton and atmospheric e^\pm and γ -background components at the level of ATIC flights ($\sim 5\text{g}/\text{cm}^2$) [1] and energies more than 50 GeV have an energy spectral power index $\gamma_A \simeq -2.7$ and could change significantly the observed spectral index $\gamma_e \simeq -3.2$ of Galactic electrons, especially above the TeV energy region, where an exponential energy cut-off is expected [19].

ATIC, the acronym for Advanced Thin Ionization Calorimeter was designed for multiple, long duration balloon flights, to measure nucleonic cosmic ray spectra from

10 GeV to near 100 TeV total energy, using a fully active Bismuth Germanate (BGO) calorimeter. It was equipped with the first large area mosaic of small fully depleted silicon detector wafers for charge identification of cosmic rays from H to Fe. As a particle tracking system, three projective layers of x-y scintillator hodoscopes were employed, above, in the center and below a Carbon interaction target[11]. The experiment had no magnetic field and was designed for cosmic ray elemental composition measurements with limited particle ID (PID) capability especially for the types of measurements mentioned in reference [1].

In this letter, we used the published data of reference [1] and applied their cut parameters, without delving into a detailed analysis of their validity, to a GEANT Monte Carlo (MC) [12]. The primary energy nuclei spectra were taken from power law approximations of balloon and satellite data [14]

$$\frac{d\mathfrak{S}_A}{dE_A} = \Phi_A E_A^{-\gamma_A}, \quad (1)$$

where Φ_A and γ_A are the scale parameters and spectral indices for $A \equiv p, He, O$ -like, and Fe -like nuclear species [14].

The flux of the p, e^\pm and γ -background components of cosmic rays at the ATIC level were computed using CORSIKA shower simulation code [15] in the frames of SIBYLL [16] interaction model, taking into account the South Pole atmosphere and magnetic field. The estimated contributions of the secondary atmospheric γ and e^\pm -components to the Galactic electron flux varied slightly from the corresponding ATIC results of reference [1]. Because of their negligible contribution to the overall data, we have omitted the details here and instead concentrate on the main background which comes from cosmic ray protons.

The contribution of the primary proton background to the Galactic electron flux was calculated using the proton spectra at the ATIC level in a GEANT-3.21 calculation with the GCALOR routines in the frame of the FLUKA interaction model for the ATIC detector [13]. This calculation takes into account the ATIC geometry with the silicon matrix, scintillator hodoscopes, graphite targets and eight layers of x-y BGO crystals, containing appropriate material compositions [11]. The total number of

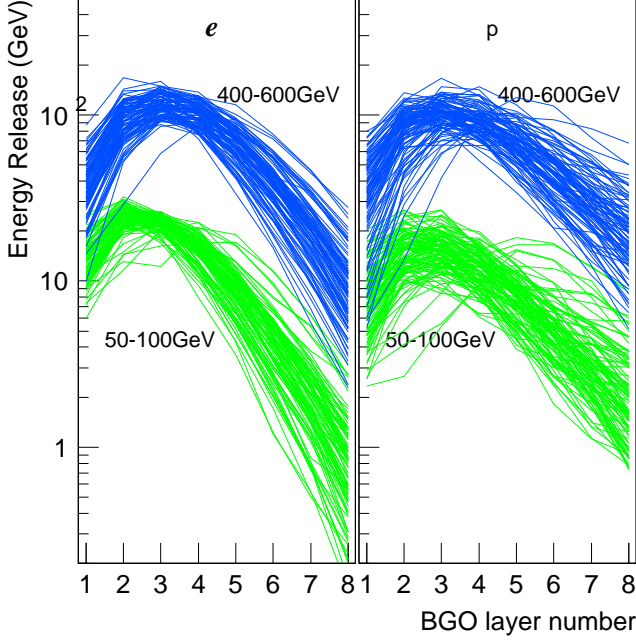


FIG. 1: GEANT simulated electron (left panel) and proton (right panel) cascade longitudinal profiles in the ATIC BGO calorimeter at energies of 400 – 600 GeV (upper lines) and at 50 – 100 GeV (lower lines).

simulated proton and electron events were 100,000 and 10,000, respectively.

These GCALOR calculations for the ATIC detector were previously compared with a FLUKA-2006 calculation [17] as well as with those of an ATIC test-beam run at CERN [18]. Furthermore, we also ran FLUKA-2006 for the ATIC configuration and results were consistent with those of the GCALOR calculations. Figure 1 shows the electron (left panel) and proton (right panel) induced cascade profiles in the ATIC BGO calorimeter after e -like cascade selection criteria: $n_{\max} \leq 5$, $E_{d,\max} > E_{d,\max+1} > E_{d,\max+2} \dots E_{d,8}$, $E_{d,1} > 2$ GeV and $E_{d,8} > 25$ MeV, where $E_{d,n}$ is the detected energy in the n -th BGO layers and $E_{d,\max} = \max(E_{d,n})$ for $n = 1, \dots, 8$. The lower and upper lines in Figure 1 correspond to 50 – 100 GeV and 400 – 600 GeV detected energies respectively. The selection criteria rejects 74% of proton events with visible energies $E_v > 50$ GeV without significant change of the electron cascade detection efficiency. This result is in close agreement with the e -cascade selection efficiency ($\sim 90\%$) and proton rejection efficiency ($\sim 75\%$) of reference [1].

We simulated the lateral distribution of the cascade parameter $F \equiv \sigma_1 + \sigma_2 + F_7 + F_8$ employed in reference [1] for proton induced e -like cascades and pure e -cascades. Figure 2 shows the published data of reference [1] and our calculations. Note the indices of σ

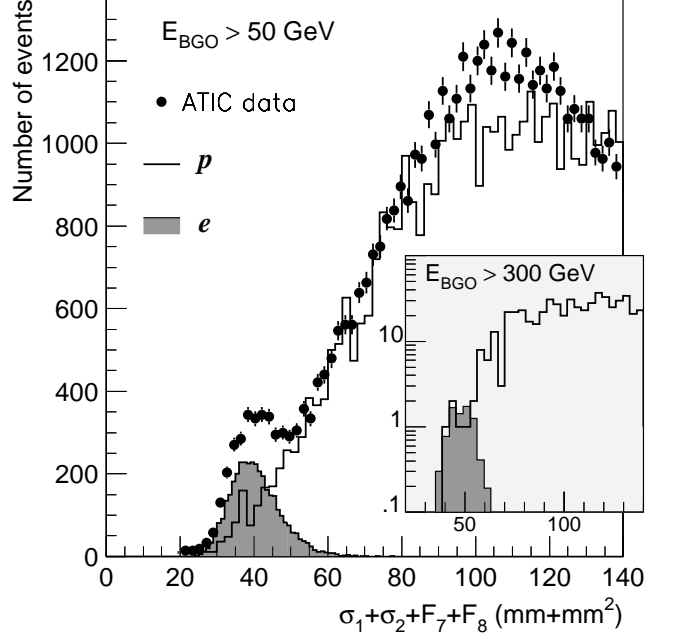


FIG. 2: Distribution of combined cascade parameter $\sigma_1 + \sigma_2 + F_1 + F_2$ for detected energies $E_{BGO} = E_d > 50$ GeV (and 300 GeV, inset histograms). The symbols are the ATIC data from [1]. The large (line) and shaded histograms are the expected distributions for primary proton and electron passing through the BGO calorimeter.

and F refer to the BGO layers. Our simulated data for $E_v > 50$ GeV was normalized to the corresponding statistics of the ATIC data [1] taking into account energy-dependent ratio $(d\mathfrak{S}_p/dE_p)/(d\mathfrak{S}_e/dE_e)$ of the expected proton flux from expression (1) and the expected electron flux ($d\mathfrak{S}_e/dE_e = \alpha E_e^{3.05} \exp(-E_e/E_0)$) from the HESS experiment [19]. The results of the GEANT simulations for visible energies $E_v > 300$ GeV are shown in the inset histogram, as well.

It is observed that the contribution of primary proton induced e -like cascades in the ATIC BGO calorimeter to the flux of Galactic electrons is quite substantial in the region of the reported excess ($E_d > 300$ GeV). [1]. "Pure" e -cascade pattern recognition in the ATIC data is performed using diagonal energy dependent cuts [1] in a 2-dimensional (2d) $(\sigma_1 + \sigma_2, F_1 + F_2)$ space. The corresponding GEANT simulated $((\sigma_1 + \sigma_2), E_d)$ and $((F_7 + F_8), E_d)$ scatter plots are presented in Figure 3. The number of simulated events was taken to be equal at 5000 events for both electrons and protons with $E_d > 50$ GeV. Note that the actual ratio of p/e in cosmic rays is approximately 300-500 for these energies.

Because the 2d selection criteria (cuts) applied in the published data were unavailable from the literature, we derived these 2d cuts (lines in Figure 3) from the GEANT

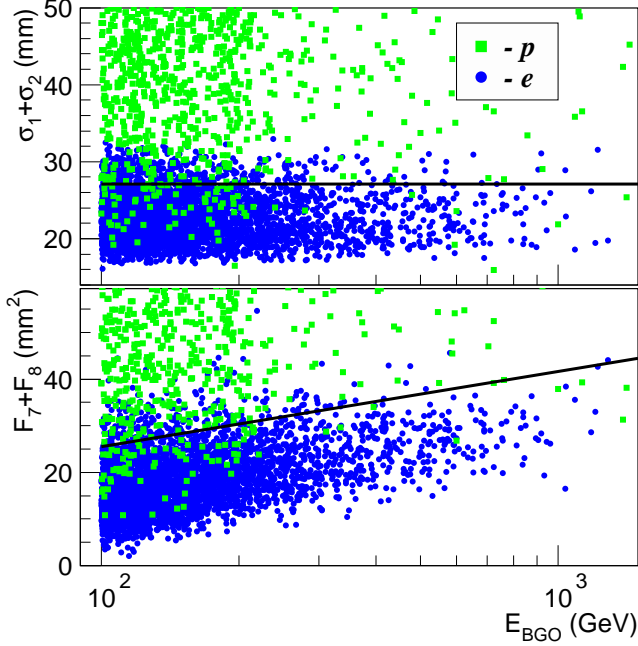


FIG. 3: 2-dimensional $((\sigma_1 + \sigma_2), E_{BGO})$, (upper panel) and $((F_7 + F_8), E_{BGO})$, (lower panel) scatter plots for 5000 simulated proton and electron events in the ATIC BGO calorimeter. The lines are the corresponding proton rejecting cuts.

simulated database using known 84% efficiency of e -cascade selection from [1]. Lines shown in Figure 3 represent cuts corresponding to the same afore-mentioned selection efficiency of e -cascade from GEANT simulated database.

The energy spectrum of proton induced and subsequent misidentified e -like events expected in the ATIC data were calculated according to the expression

$$F_{p-e} = \frac{\mathfrak{F}_p}{N_{tot}} \frac{\Delta N}{\Delta E \cdot \delta_e \cdot \xi} \quad (2)$$

where $E_e = E_d/\varepsilon$ and ε is the average fraction of released energy due to e -cascade passing through the BGO calorimeter [1], \mathfrak{F}_p is the integral energy spectrum of the primary protons from expression (1) for $E_{p,min} = 100$ GeV, N_{tot} is the total number of simulated proton events, ΔN and ΔE are the number of selected e -like proton induced events in the given ΔE energy bin, $\delta_e = 0.84$ [1] is the efficiency of 2-dimensional e -cascade selection cuts, and $\xi(E_e) \simeq \xi \equiv \mathfrak{F}_{e,ATIC}/\mathfrak{F}_{e,Prim} \simeq 0.78$ is the atmospheric reduction factor taken from reference [20]. The corresponding results are presented in Figure 4 (black circles) in comparison with published data of reference [1] (black star symbols). The accuracy of the obtained energy spectrum was improved using the derivative of the corresponding integral spectra due to *a priori* known spectral index ($\gamma_p = -2.75$) of proton induced e -like cas-

cases. The corresponding differential energy spectrum are shown in Figure 4 (black line with blue-shaded area for the expected errors), as well. Red star symbols are the residual energy spectrum of Galactic electrons after subtraction of the expected proton induced e -like cascade from the reported data of reference [1].

In summary, Figure 4 clearly shows that the MC pro-

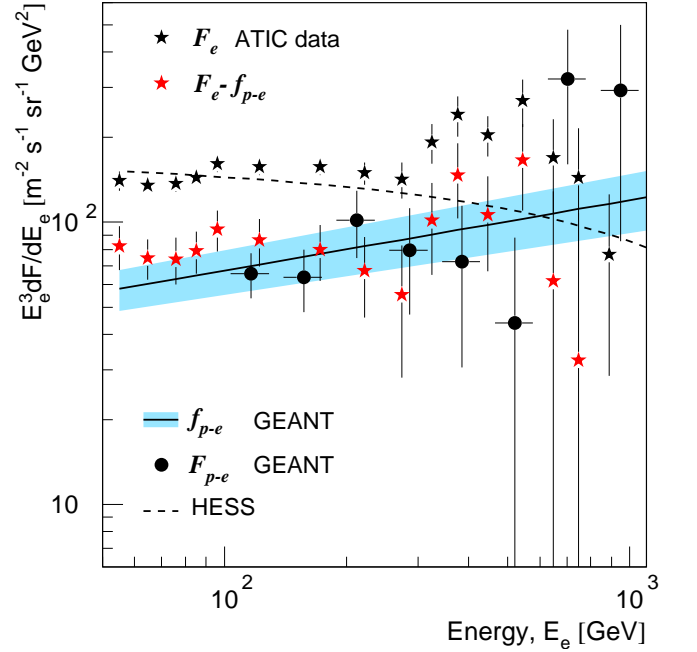


FIG. 4: Galactic electron and misidentified e -like energy spectra. The solid black stars (F_e) are the data of reference [1], the red stars are the ATIC data after subtraction ($F_e - f_{p-e}$) of e -like proton energy spectrum (f_{p-e} , the solid line with blue shaded area of errors) obtained from the corresponding integral flux, the solid black circles are the GEANT simulated proton induced e -like events energy spectrum. The dashed line is the power law energy spectrum with exponential cut-off from HESS [19].

ton spectrum has a substantial contribution in the energy region of more than 300 GeV where an excess of e -like events was reported [1]. Our analysis indicates that a calorimeter such as ATIC with its limited PID capability could easily misidentify protons for electrons and thereby yield unwarranted physics conclusions. We conclude that the contribution from cosmic ray protons at energies above 300 GeV has not been properly included in reference [1]. This analysis shows that the results of reference [1] does not merit any exotic conclusion and that the electron spectrum is consistent with that reported by the AMS collaboration [21].

The authors gratefully acknowledge a grant from NASA under the contract No. NNX07AE49G.

* Electronic address: ali.fazely@subr.edu

† Present address: Box 3155, Duke University Medical Center, Durham, NC 27710

- [1] J. Chang, *et al.*, Nature (London) 456, 362 (2008).
- [2] Juan Zhang, *et al.*, arXiv:0812.0522v2 [astro-ph] (2008).
- [3] Ilias Cholis, *et al.*, arXiv: 0811.3641 [astro-ph] (2008).
- [4] Koji Ishiwata, *et al.*, arXiv: 0903.0242v1 [hep-ph] (2009).
- [5] Hong-Bo Hu, *et al.*, arXiv: 0901.1520 [astro-ph] (2009).
- [6] Nir J Shaviv, *et al.*, arXiv: 0902.0376v1 [astro-ph] (2009).
- [7] Stefano Profumo, arXiv: 0812.4457v1 [astro-ph] (2008).
- [8] A.W. Strong and I.V. Moskalenko, Adv. Space Res. 27 (2001) 717.
- [9] Simon Swordy, Proc. 28th ICRC, Tsukuba, Japan 1989 (2003).
- [10] Igor V. Moskalenko *et al.*, arXiv: astro-ph/0402243v1 (2004).
- [11] T.G. Guzik, *et al.* Advances in Space Res. **33**, 1736 (2004).
- [12] <http://wwwasd.web.cern.ch/wwwasd/geant>
- [13] C. Zeitnitz, T.A. Gabriel, Nucl. Inst. Meth. **A349** 106(1994).
- [14] B. Wiebel-Sooth, P.L. Biermann, H. Meyer, Astron. Astrophys. **330**, 389 (1998).
- [15] D. Heck, J. Knapp, J.N. Capdevielle, G. Schatz, T. Thouw, Forschungszentrum Karlsruhe Report, FZKA 6019 (1998).
- [16] R.S. Fletcher, T.K. Gaisser, P. Lipari, T. Stanev, Phys.Rev. **D50** (1994) 5710.
- [17] R.M. Gunasingha, *et al.*, 30th ICRC Merida, Mexico **2** 75 (2007).
- [18] A. Naqvi, MSc Thesis, Southern University (2001) Unpublished.
- [19] F. Aharonian *et al.* (HESS collaboration), arXiv: 0811.3894v1 [astro-ph] (2008).
- [20] J. Chang, *et al.*, 29th ICRC, Pune, India **3** 1 (2005).
- [21] M. Aguilar, *et al.*, Physics Reports **366**, 331 (2002).